ACS APPLIED MATERIALS & INTERFACES

Research Article

Cite This: ACS Appl. Mater. Interfaces XXXX, XXX, XXX−XXX

www.acsami.org

Effect of Ambient Chemistry on Friction at the Basal Plane of Graphite

Arash Khajeh,[†] Zhe Chen,[‡] Seong H. Kim,*[,‡] and Ashlie Martini*[,†]

[†]Department of Mechanical Engineering, University of California Merced, 5200 N. Lake Road, Merced, California 95343, United States

[‡]Department of Chemical Engineering and Materials Research Institute, Pennsylvania State University, University Park, Pennsylvania 16802, United States

Supporting Information

ABSTRACT: Graphite is widely used as a solid lubricant due to its layered structure, which enables ultralow friction. However, the lubricity of graphite is affected by ambient conditions and previous studies have shown a sharp contrast between frictional behavior in vacuum or dry environments compared to humid air. Here, we studied the effect of organic gaseous species in the environment, specifically comparing the adsorption of phenol and pentanol vapor. Atomic force microscopy experiments and reactive molecular dynamics simulations showed that friction was larger with phenol than with pentanol. The simulation results were analyzed to test multiple hypotheses to explain the friction difference, and it was found that mechanically driven chemical bonding between the tip and phenol molecules plays a critical role. Bonding increases the number of phenol molecules in the contact, which increases the adhesion as well as the number of atoms in registry with the topmost graphene layer acting as a pinning site to resist sliding. The findings of this research provide insight into how the chemistry of the operating environment can affect the frictional behavior of graphite and layered materials more generally.

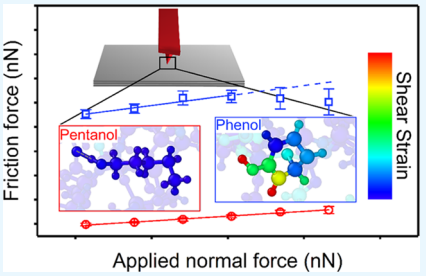

KEYWORDS: *friction, graphite, organic molecules, atomic force microscopy, reactive molecular dynamics simulations*

INTRODUCTION

Graphite is used as a solid lubricant in many applications due to its excellent tribological performance. Ideally, graphite solid lubricants could function across a wide range of environmental conditions. Unfortunately, ultralow friction is not an intrinsic property and many previous studies have shown that the lubricity of graphite is highly sensitive to the environment.[1] Macro- and microscale measurements have shown that friction on graphite is relatively high in vacuum or dry nitrogen[2,3] but can be decreased significantly by the presence of gaseous species including water and oxygen.[2,4] The same trends have been observed in nanoscale experiments based on atomic force microscopy (AFM)[5−10] as well as atomic-scale simulations.[5−7,11−14]

Nanoscale studies have suggested multiple mechanisms for the environment-dependent friction of graphite. Most of these mechanisms are centered around the physical and chemical interactions between gas-phase species in the environment and atomic-scale defects on the graphite surface.[5,8−11,14,15] AFM and nanoindentation studies suggested that friction of graphite in dry conditions can increase due to interactions between the tip and defects on the graphite surface generated during sliding.[9,10] In this context, the role of water molecules is to neutralize dangling bonds and reduce the covalent bond formation in the interface, thus decreasing the probability of wear and associated friction.[9,10] These experiments were supported by density functional theory (DFT) calculations, which showed that water molecules are physisorbed on the basal plane of graphite and chemisorbed at point defects like vacancies.[11,14] Further, lower friction achieved with a hydrophobic tip compared to a hydrophilic tip showed that chemical interactions between the AFM tip and graphite surface also contribute to friction.[8,15] Other studies that did not consider defects attributed environment effects to physisorption. A recent study[6] using AFM complemented by molecular dynamics (MD) simulations suggested an intrinsic friction hysteresis mechanism related to the motion of water molecules across the graphene basal plane that strongly depends on both humidity and hydrophobicity of graphite basal plane. This study attributed friction hysteresis between loading and unloading in a humid environment to changing contact angles due to physisorbed water on the graphite. Grand Canonical Monte Carlo simulations and AFM experiments[5] showed that friction varied nonmonotonically with humidity and that this trend could be explained by the physisorption of water in the contact region that affected the quality of the contact. However, the hypothesis of water adsorption on the basal plane of graphite may not fully explain the observed humidity dependence of friction because a recent study measuring the water adsorption isotherm on a freshly exfoliated graphite

Received: July 26, 2019
Accepted: October 3, 2019
Published: October 3, 2019

DOI: 10.1021/acsami.9b13261
ACS Appl. Mater. Interfaces XXXX, XXX, XXX−XXX

surface showed that water adsorption does not occur readily until the humidity approaches the saturation point.[16]

Most studies mentioned above compared vacuum or dry nitrogen with humid air environments. However, in typical ambient conditions, chemical species other than water and oxygen are present, for example, organic molecules. Further, graphitic surface coatings[17] and lubricant additives[18−20] may be exposed to hydrocarbons and their derivatives in lubricating oils. Vapor phase lubrication studies at the macroscale showed that hydrocarbons have a more significant effect on lubricity than water since they require lower relative partial pressure than water for effective lubrication.[21] These experiments suggested that molecular species adsorbed on the graphite basal plane can act as a reservoir from which the molecules can migrate to and neutralize defect sites during the sliding process. Further, it was shown that the lubricity of alcohols and alkanes on graphite improves with increasing molecular size, since adsorption energy increases with molecular chain length.[21]

Previous MD simulations have investigated the effect of organic species on graphite friction.[12,13,22−26] Among these studies, simulations suggested that the energy barrier for lateral translation and molecular mobility of benzene and C60 molecules on a graphite basal plane was dependent on the rotational degree of freedom of these species.[13,12,26] These results suggested that the friction force and energy barrier required for sliding could be attributed to the mobility of molecules present on the graphite surface, which is determined by the structure of the species and temperature. However, these studies assumed that the behavior of the molecules could be explained by physisorption, and the possible effects of chemical bonding in the interface were not considered.

In the present study, we performed friction experiments using AFM along with reactive MD simulations of a silica AFM tip sliding on a graphite basal plane in the presence of pentanol and phenol. Phenol (C_6H_5OH) is an aromatic compound composed of a hydroxyl group attached to a benzyl ring, and pentanol ($C_5H_{11}OH$) is an aliphatic alcohol with five carbon atoms. The selection of pentanol and phenol for this study enabled investigation of the effect of molecular structure on friction for two broad categories of hydrocarbon derivatives, namely, aromatic and linear organic molecules. Friction was measured as a function of load in both AFM experiments and MD simulations. Then, the simulations were used to test hypotheses to explain the observed friction differences by calculating the parameters including the accumulation of molecules due to physical adsorption near the contact, the registry of atoms relative to the graphite basal plane, the direction of molecular motion on the surface, and chemical bonding between the molecules and the tip. The results show that differences in the chemistry of molecules can affect friction and that the difference can be explained in the terms of covalent bonding between the organic molecules and the tip. Lastly, this bonding is correlated to the force exerted by the contacting bodies and the resulting internal strain within the molecules.

METHODS

AFM Experiments. A clean graphite surface was produced on a highly oriented pyrolytic graphite crystal through tape exfoliation in ambient air. Nanoscale friction tests were performed using an AFM system (Multimode, Bruker) with Si probes (CONTV, Bruker) in contact mode. The spring constant of the Si probe cantilever was determined with Sader's method.[27] The probe surface had a native silica layer, so it was regarded as a silica probe. The lateral sensitivity of the cantilever in this setup was obtained by comparing the measured lateral signal on a reference sample with a known coefficient of friction (COF). The reference sample was a hydrogenated diamondlike carbon coating, whose COF was about 0.15 in a pentanol vapor (40% of the saturation pressure) lubrication condition.[28] Before the friction test, the AFM probe was treated with UV/ozone for 15 min.[29] During the test, the AFM tip was rubbed against the graphite surface in a reciprocating motion. A region without graphene step edges was selected as the scan area. The stroke length was 200 nm, and the frequency was 2.5 Hz, so the relative sliding speed was 1 μm/s. Friction tests were performed in pentanol and phenol vapor environments. For the pentanol environment, a gas stream of pentanol and nitrogen was passed through the AFM chamber at a rate of 50 cm^3/min; the partial pressure of pentanol was 80% of its saturation pressure. For the phenol environment, small crystallites of phenol were put inside the AFM chamber to maintain the partial pressure of phenol near the saturation pressure. Friction was measured at an increasing applied normal load from 6.4 to 38.3 nN, and all tests were performed at room temperature (around 22 °C). The adhesive force measured from pull-off experiments was found to be 30.9 nN in dry N_2, 15.0 nN in pentanol vapor, and 43.4 nN in phenol vapor. Assuming a tip radius of 120 nm (based on the relative magnitudes of adhesive force with a 2 nm radius tip and the tip used in the friction experiments), the DMT contact model was used to calculate the contact pressures of 0.37−0.51 GPa in pentanol vapor and 0.50−0.59 GPa in phenol vapor.

MD Simulations. To complement the AFM experiments, the friction of an amorphous silica tip apex sliding over the basal plane of a graphite substrate was modeled using reactive MD simulations. The ReaxFF[30] used in this work was previously developed for the C/O/H/Si/F system[31] from a combination of parameters for C/H/O[32,33] and Si/C.[34] Although ReaxFF is known to underestimate the low-temperature reactivity of phenol compared to DFT calculations,[35−37] it has been used to explore the chemical interactions between these molecules and other materials including graphite at room temperature.[38,39] It has been also shown that ReaxFF performs adequately in its representation of graphite compressibility.[40] The amorphization of silica was performed using a heat-quench process, which consisted of heating of crystalline cristobalite to 4000 K and then cooling to room temperature at a rate of 0.02 K/fs.[41,42] Based on previous experiments, silica adsorbs organic compounds such as phenol and pentanol when they are available in the environment.[43] To mimic this adsorption while keeping the model size small for computational efficiency, the model tip surface was terminated with methoxy groups. Figure 1 illustrates the structure of pentanol (a) and phenol (b) molecules as well as the setup used in simulations (c), including the silica tip, organic molecules, and graphite substrate. The simulation was initially

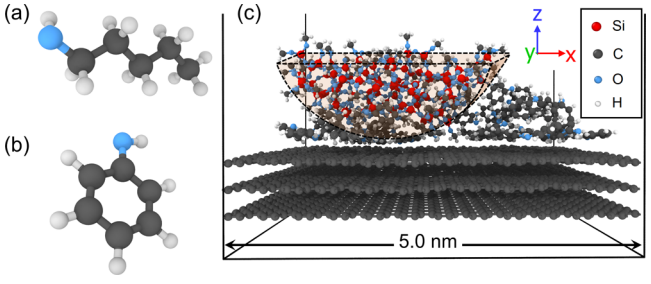

Figure 1. Snapshots of (a) pentanol, (b) phenol, and (c) the simulation of friction between a nanoscale silica probe and the basal plane of graphite in the presence of phenol. A second model is the same except phenol molecules are replaced with pentanol. The tip structure (shaded area) is amorphous silica terminated with methoxy groups to mimic a native oxidized silicon tip in the presence of organic molecules.

DOI: 10.1021/acsami.9b13261
ACS Appl. Mater. Interfaces XXXX, XXX, XXX−XXX

assembled by placing the tip at the top of the model system, the graphite substrate at the bottom and 50 pentanol or phenol molecules in the middle. To decrease the computational cost, only a three-layer graphite substrate was considered. The substrate dimensions were 5.0 nm in the sliding direction (x-direction), 4.0 nm perpendicular to the sliding direction on the basal plane (y-direction), and about 1.0 nm normal to the graphite basal plane (z-direction). The amorphous silica tip had a half-disk shape with a 3.5 nm radius in the xz-plane and 1.5 nm thickness in the y-direction. Throughout the simulation, the bottom graphene layer was fixed, and the top 0.5 nm of the tip was treated as a rigid body; all other atoms could move freely.

Each simulation consisted of four steps: (i) energy minimization and initial equilibration until a stable potential energy was reached; (ii) vertical compression of the tip toward the substrate at 10 m/s until the minimum distance between the tip and the substrate reached 0.3 nm; (iii) application of a 10, 30, or 50 nN normal load at the top rigid part of the tip for 120 ps; and (iv) sliding at 10 m/s by pulling the tip with a harmonic spring with a stiffness of 6 N/m. The adhesion forces measured from simulations of pull off tests were 3.4 and 4.3 nN for pentanol and phenol, respectively. Although the model tip was not spherical, the apparent contact area calculated from the size of a rectangle that enclosed all tip atoms within 0.3 nm of the substrate was used to approximate an effective spherical tip radius of 1.6 nm. Then, for the applied normal load range of 10−50 nN, the DMT model was used to estimate contact pressures of 5.0−8.1 GPa in both pentanol and phenol. Simulations were run in the canonical ensemble with the temperature maintained at 300 K using a Langevin thermostat applied to the unconstrained atoms. Due to the high velocity during the sliding step, the motion of the atoms in the sliding direction was excluded from the temperature calculation used by the thermostat. A 0.25 fs time step and 20 fs thermostat damping factor were used in all simulations. The friction force during sliding was calculated by monitoring the force on the tip atoms in the sliding direction. Throughout the simulations, bonds between atoms were identified as those with a bond order of 0.3 or larger. All the simulations were performed using the large atomic/molecular massively parallel simulation code,[44] and OVITO software[45] was used to visualize the results.

RESULTS AND DISCUSSION

Figure 2a reports the mean friction force as a function of normal load from AFM experiments performed in pentanol and phenol vapor conditions. These results show that, within the range of applied normal loads tested, there is a higher friction between the sliding AFM tip and graphite substrate in phenol compared to that in pentanol. The standard deviation (STDEV) of the friction force collected in one scan (512 data points in a trace or retrace scan) is shown in Figure 2b, and it is also higher for phenol than for pentanol. The mean and STDEV of the friction force at different applied normal loads in the MD simulations are shown in Figure 2c,d, respectively. In the simulations, the difference between the mean friction forces for pentanol and phenol is not as large as that observed in the experiments. However, the STDEV of the friction signal is significantly higher for phenol than for pentanol in the simulations. The raw friction data from the simulations with pentanol and phenol at the 10 nN load are shown in Figure S1a,b and illustrate the larger force fluctuations for phenol, particularly after about 2 nm of sliding. It has been previously proposed that the STDEV of the lateral force can be used as a measure of frictional energy dissipation.[46] Therefore, both mean and standard deviation of the force are relevant to the comparison between phenol and pentanol; as shown in Figure 2, both are larger for phenol in experiments and simulations.

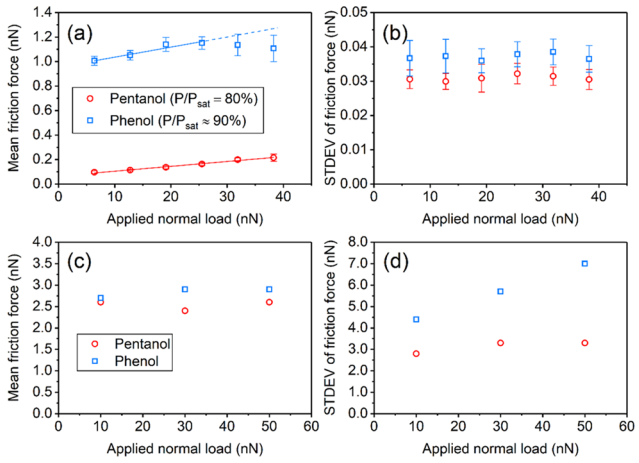

Figure 2. Mean (a, c) and standard deviation (b, d) of the friction force for a silica AFM tip sliding on the graphite basal plane in the presence of pentanol and phenol vapor from AFM experiments (a, b) and MD simulations (c, d). The error bars in (a) and (b) correspond to the deviation across different scans.

Although simulations and experiments exhibit similar trends, there are differences in magnitudes that are attributable to the substantial differences in the contact size and sliding speed. For example, the smaller STDEV in the experiments can be explained by the significantly larger tip size, which makes the system more stable compared to the simulation setup. Also, since atomic-scale friction is known to increase with applied pressure and sliding speed,[47,48] the higher mean friction in the simulations may be partially explained by much higher pressures and speeds in the simulations compared to the experiments. Nonetheless, the qualitative trends are the same in both AFM and MD results, i.e., both indicate larger mean friction and STDEV for phenol.

As a reference, a simulation of dry sliding was performed without molecules; the result was considerably smaller friction force fluctuations (see Figure S1d). This indicates that the organic species are directly responsible for the observed friction trends. Also, the simulations at 10 nN load were repeated with 60 pentanol molecules (as opposed to 50) to match the number of carbon atoms in the phenol system, and the same STDEV was obtained, as reported in Figure S1c. Therefore, the friction difference between phenol and pentanol is attributable to the chemistry of the molecules rather than the number of atoms they contain.

The effect of environment on friction for graphite is typically attributed to the physical and chemical adsorption of species at defects such as step edges or vacancies.[9,10,49,50] However, the simulations here describe an ideal graphite basal plane, so those explanations are not applicable in this case. Other hypotheses that might explain the difference between friction with phenol and pentanol are: (i) accumulation of molecules due to physical adsorption at the tip−surface interface;[8,15] (ii) differences in commensurability between molecular species being dragged inside the contact area with one of the two sliding bodies;[5] or (iii) tribochemical reactions happening at the sliding interface.[51] Each of these hypotheses was tested through the simulations.

To investigate the first hypothesis, the positions of the molecules were analyzed during the sliding simulations. At the beginning of simulation, the molecules were distributed across the surface at a vertical position between the top layer of graphene and the bottom of the tip. During the equilibration step, the molecules approached the surface and physisorbed to

DOI: 10.1021/acsami.9b13261
ACS Appl. Mater. Interfaces XXXX, XXX, XXX−XXX

the graphite basal plane (Figure S2). After the tip was brought into contact and sliding began, these molecules remained on the surface, as shown in the representative snapshots in Figure S3. To directly compare phenol and pentanol, the positions of physisorbed carbon atoms along the sliding direction were averaged over the last 2 nm of sliding (the steady-state region, based on trends in Figure S1b). As shown in Figure S4, there were more carbon atoms in the contact area and in front of the tip with phenol than with pentanol. This difference may contribute to the greater friction observed with phenol.

The effect of commensurability was explored by characterizing the registry index (RI)[52,53] of atoms at the interface. RI is usually employed to study the tribological properties of solid interfaces with different crystal lattices. For example, for a bilayer graphene interface, the most energetically favorable position for a carbon atom is above the middle of the hexagon of carbon atoms in the adjacent layer; this position corresponds to an RI of 0. In the other limiting case, where a carbon atom is directly above another carbon atom in an adjacent layer, the RI is 1. Intermediate positions correspond to RI values between 0 and 1, where a lower RI indicates a more energetically favorable position. Here, the RI was calculated for individual carbon atoms in the molecules relative to the carbon atoms in the graphite basal plane, where a smaller RI corresponds to a greater commensurability between an adsorbate atom and the topmost surface of graphite. The RI values were averaged over the last 2 nm of sliding for both phenol and pentanol. As shown in Figure 3a,

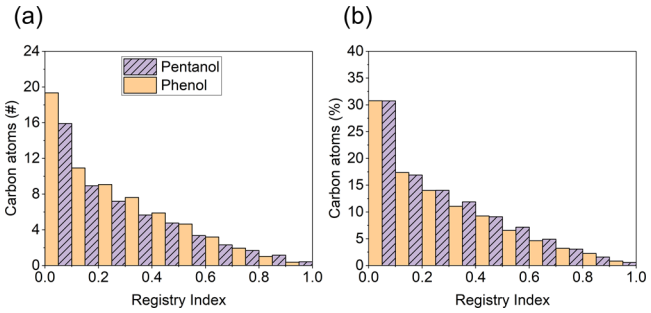

Figure 3. (a) Histograms of the RI for carbon atoms in the molecules with respect to carbon atoms on the topmost layer of the graphite averaged over the last 2 nm of sliding. The RI is higher for phenol than for pentanol, but this difference is not observed when (b) the data are normalized by the number of atoms in the contact area.

there were more phenol atoms with low RI than pentanol atoms. Based on previous studies,[5] atoms with low RI at the interface can act as pinning sites and contribute to friction during the sliding process. The observed difference in RI is unlikely to be due to stronger interactions between the phenol and the surface vs the pentanol since the $\pi-\pi$ interactions between the benzene ring and the surface are relatively weak (comparable to thermal energy at room temperature). Further, after normalizing the RI by the total number of carbon atoms in the contact area, as shown in Figure 3b, no difference between pentanol and phenol molecules was observed. Therefore, there are more pinning sites in the case of phenol, but this is explained by the larger number of molecules in the contact as opposed to the positions of those molecules on the surface.

The trajectories of the molecules are illustrated by the positions of the oxygen atoms during sliding in Figure 4 and

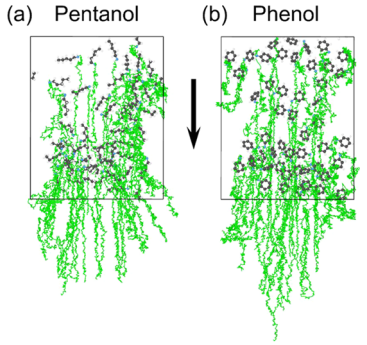

Figure 4. Top view of the trajectories of oxygen atoms in (a) pentanol and (b) phenol molecules (indicated by green lines) during the sliding process. The molecules shown in the figures represent their positions before sliding. The trajectories are longer in the sliding direction (arrow in figure) for phenol, indicating that these molecules are being dragged in the contact by the tip, while pentanol molecules can escape out from the sides of the contact.

provide information about the motion of pentanol and phenol molecules in the simulation. Comparing two cases, it can be observed that there are many short and inclined trajectories diverging from the sliding direction in the case of pentanol, while there are longer trajectory lines along the sliding direction in the case of phenol. These observations suggest that pentanol can escape the contact area while phenol molecules are dragged along with the tip. This is consistent with previous experiments[54−56] and classical MD simulations[57,58] that compared linear and cycloaromatic hydrocarbons and showed that the greater flexibility of the linear hydrocarbons enabled them to more easily slide relative to one another and escape the contact area.[58] However, physical mechanisms may not fully explain the mobility of the phenol and pentanol in our simulations.

Although the graphite surfaces remained intact and unreactive throughout the simulations, covalent and hydrogen bonds between the tip and molecules were observed. Snapshots of the simulation illustrating representative bonds that were observed are shown in Figure 5. In the case of pentanol, only hydrogen bonds were observed between the molecules and the tip. However, for phenol, we observed $Si_{tip}-C_{phenol}$ and $O_{tip}-C_{phenol}$ covalent bonds. This observation is not surprising since the aromatic ring in phenol is considerably

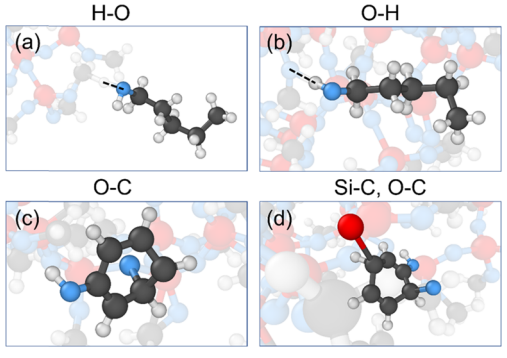

Figure 5. Snapshots showing examples of bonding between the molecules and the tip. Pentanol interacts with the tip primarily via hydrogen bonds (a, b) while phenol exhibits covalent bonding with the tip (c, d). All atoms not involved in the bonds being emphasized are shown as faded.

DOI: 10.1021/acsami.9b13261
ACS Appl. Mater. Interfaces XXXX, XXX, XXX−XXX

more reactive than the aliphatic alcohol chain due to the activation of the benzene ring by the attached hydroxyl group.[59,60]

The tip−molecule bonding during the simulation was quantified as the number of bonds vs time. As shown in Figure 6a,b for the simulations performed at the applied

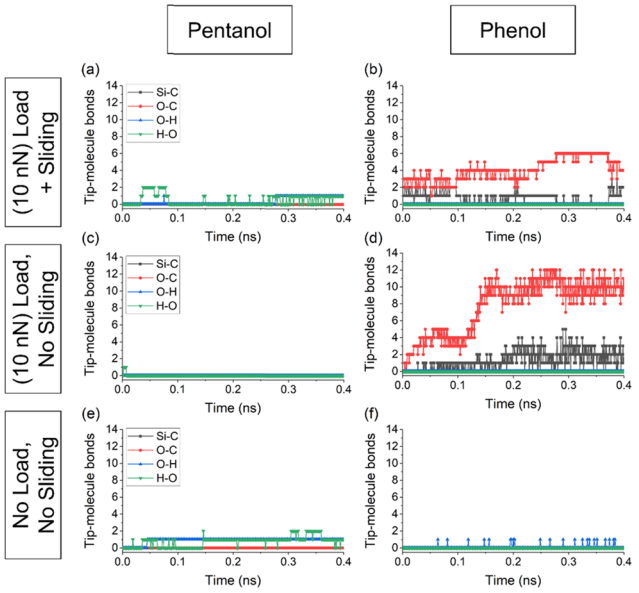

Figure 6. Number of bonds between the tip and molecules as a function of time for each atom−atom pair, where the first element corresponds to an atom in the tip and the second is in the molecule, from simulations with 10 nN load and sliding (a, b), 10 nN load only (c, d), and with no load (e, f). Few bonds are observed under any condition with pentanol (a, c, e). However, with phenol, the load and sliding cases (b, d) exhibit bonding, suggesting that bond formation is driven by mechanical forces exerted on the molecules in the contact.

normal load of 10 nN, there were more tip−phenol bonds than tip−pentanol bonds. The pentanol exhibits few and short-duration hydrogen bonds during the simulation, while phenol forms $O_{tip}-C_{phenol}$ and $Si_{tip}-C_{phenol}$ bonds that persist throughout the simulation. To understand this difference, simulations were repeated without load or sliding and with load but no sliding. As shown in Figure 6c,e, tip−pentanol bonding was not observed for any load or sliding condition. However, the simulations of phenol with applied normal load only and without load or sliding (Figure 6d,f) showed that covalent bonds were observed only when load was applied. The number of bonds was averaged over the last 0.1 ns of the simulation at all three loads and the results are shown in Figure S5. Higher loads did not increase the bonding with pentanol but, except for the $O_{tip}-C_{phenol}$ bonds at 10 nN, the number of covalent bonds between phenol and the tip increased with load.

The fact that the covalent bonds are only observed when the normal load is applied suggests that the chemical reactions between the tip and phenol molecules are driven by the mechanical force in the contact. Both experiments[61,42] and numerical studies[42,51,62] have previously reported mechano-chemical reactions during the sliding process. Note that there are more tip−phenol covalent bonds during loading (Figure 6d) than during sliding (Figure 6f). This can be attributed to the movement of phenol molecules away from the contact during the sliding process, as observed in Movie S1, such that there are fewer opportunities for tip−phenol bonding in the short duration of the simulation. In the case of load only, the molecules are trapped in the contact region (Movie S2) where they can then bond with the tip.

To understand how mechanical force drives tip−phenol bonding, the atomic shear strain[63,64] was quantified as the change in the positions of neighboring atoms within a 0.25 nm radius with respect to their position at the beginning of the equilibrium step. Figure 7a−d illustrates the shear strain of

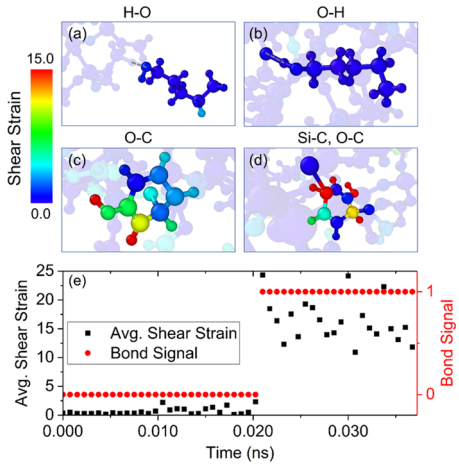

Figure 7. (a−d) Atomic shear strain on representative molecules bonded to the tip (same molecules as in Figure 5). Pentanol molecules experience negligible shear strain, while phenol molecules bonded to the tip experience a significant amount of shear deformation. (e) Shear strain and bond status (0 = no bond; 1 = bond) for a carbon atom in the aromatic ring of a phenol molecule during the load application step (a 10 nN load is applied at time zero).

representative molecules after bonding to the tip during the sliding process; these are the same molecules that are shown to interact with the tip in Figure 5. These snapshots show that pentanol molecules (a and b) experience a much less internal strain than phenol molecules (c and d). Also, since phenol−tip bonding was only observed in simulations with load (see Figures 6 and S5), this result suggests that the normal load that causes shear strain is responsible for the interfacial bond formation, and that this process may be facilitated by the deformation of the molecule.

To confirm the role of applied load, the atomic shear strain for a carbon atom in a representative phenol molecule was characterized during the load application step. Figure 7e shows the change in atomic shear strain and the bond status with time, starting at the point when the normal load is first applied to the tip. Initially, the shear strain on the carbon atom is negligible and is only due to thermal vibration of atoms. Then, the shear strain increases gradually until, at 0.02 ns, it increases rapidly. This moment is coincident with the formation of a covalent bond between the carbon atom in the aromatic ring of phenol and an oxygen atom in the tip. The other phenol atoms that bond to the tip exhibit similar trends. These findings confirm that the role of applied load is to strain the molecule, which facilitates covalent bond formation. This is consistent with the previous finding reported for mechanochemical reactions of allyl alcohol and α-pinene molecules at tribological interfaces of silicon oxide.[42,65] Further, since neither strain nor covalent bonding is observed with pentanol, these results show

DOI: 10.1021/acsami.9b13261
ACS Appl. Mater. Interfaces XXXX, XXX, XXX−XXX

that the susceptibility of a molecule to mechanochemical reactions is dependent on its structure.[66,67]

The mechanically driven chemisorption of phenol to the counter-surface is directly related to the observed friction trends. The covalent bonds are strong enough to drag the phenol molecules during sliding (Figure 4), which explains the presence of more phenol in the contact area (Figure S4) that can act as pinning sites resisting sliding (Figure 3). The covalently bonded phenol atoms also increase adhesion, as observed in both simulations and experiments. Taken together, these effects result in larger friction when sliding in a phenol compared to pentanol environment.

CONCLUSIONS

In this study, we employed AFM experiments and reactive MD simulations to explore the friction behavior of an amorphous silica tip sliding on a graphite basal plane in the presence of phenol and pentanol. The mean and STDEV of the friction force in both simulations and experiments were larger with phenol than with pentanol. The STDEV of the friction force was used as a measure of energy dissipation for these two systems. To understand the observed friction trends, the simulations were used to calculate parameters that could affect friction, including the number of atoms in the contact area, the RI of the atoms in the molecules on the graphite surface, the motion of the molecules, and chemical bonding between the molecules and the tip. All of these were found to be different for phenol and pentanol, and the results indicated that there were more phenol molecules in the contact that moved along with the tip and were in registry with the graphite, thereby increasing the adhesion and friction. This observation was explained by the presence of covalent bonding between phenol molecules and the tip that was not exhibited in pentanol. Further, simulations performed at different loads showed that phenol−tip bonding was driven by mechanical forces in the contact. The role of applied force was explained by the shear deformation of the phenol molecules. Overall, this study provides insight into the effect of the chemistry of the environment on the friction for an ideal graphite surface. The results illustrate how differences in the structure of organic molecules can affect their susceptibility to strain and therefore mechanochemical bonding in a sliding contact, which, in turn, affects the number of species in the contact area leading to different friction behavior. More generally, this study demonstrates that chemistry can contribute significantly to frictional sliding on graphite even in the case of an ideal surface without defects. This observation has important implications for applications that rely on graphite for lubrication in varying environmental conditions, where chemical as well as physical factors will contribute to sliding resistance.

ASSOCIATED CONTENT

Supporting Information

The Supporting Information is available free of charge on the ACS Publications website at DOI: 10.1021/acsami.9b13261.

Simulation results including friction force over time; histograms of atom positions before and after equilibration; representative snapshots of molecules on the surface; distribution of atom positions along the sliding direction and perpendicular to sliding direction; and load dependence of the average number of tip−molecule bonds (PDF)

Two animations show top-views of the phenol molecules during simulations of the tip sliding or the tip subject only to normal load. In both movies, the trajectories of the phenol molecules are represented by green lines, the boundary of the periodic model domain is shown in black, and the position of the tip is captured by shape that approximates the size of the contact region (MP4) (MP4)

AUTHOR INFORMATION

Corresponding Authors

*E-mail: shkim@engr.psu.edu (S.H.K.).
*E-mail: amartini@ucmerced.edu (A.M.).

ORCID

Arash Khajeh: 0000-0002-9061-9370
Ashlie Martini: 0000-0003-2017-6081

Notes

The authors declare no competing financial interest.

ACKNOWLEDGMENTS

This work was supported by the National Science Foundation (Grant Nos. CMMI-1727356 and 1727571).

REFERENCES

(1) Chen, Z.; He, X.; Xiao, C.; Kim, H. S. Effect of Humidity on Friction and Wear—A Critical Review. *Lubricants* **2018**, *6*, No. 74.
(2) Bryant, P. J.; Gutshall, P. L.; Taylor, L. H. A Study of Mechanisms of Graphite Friction and Wear. *Wear* **1964**, *7*, 118−126.
(3) Buckley, D. H. *Friction, Wear, and Lubrication in Vacuum*; National Aeronautics and Space Administration: Washington, D.C., 1971.
(4) Gao, X.; Chen, L.; Ji, L.; Liu, X.; Li, H.; Zhou, H.; Chen, J. Humidity-Sensitive Macroscopic Lubrication Behavior of an as-Sprayed Graphene Oxide Coating. *Carbon* **2018**, *140*, 124−130.
(5) Hasz, K.; Ye, Z.; Martini, A.; Carpick, R. W. Experiments and Simulations of the Humidity Dependence of Friction Between Nanoasperities and Graphite: The Role of Interfacial Contact Quality. *Phys. Rev. Mater.* **2018**, *2*, No. 126001.
(6) Ye, Z.; Egberts, P.; Han, G. H.; Johnson, A. T. C.; Carpick, R. W.; Martini, A. Load-Dependent Friction Hysteresis on Graphene. *ACS Nano* **2016**, *10*, 5161−5168.
(7) Egberts, P.; Ye, Z.; Liu, X. Z.; Dong, Y.; Martini, A.; Carpick, R. W. Environmental Dependence of Atomic-Scale Friction at Graphite Surface Steps. *Phys. Rev. B* **2013**, *88*, No. 035409.
(8) Jradi, K.; Schmitt, M.; Bistac, S. Influence of the Surface Chemistry on the Nanotribological Behaviour of (AFM tip/graphite) Couples. *Appl. Surf. Sci.* **2012**, *258*, 4687−4697.
(9) Stempflé, P.; Castelein, G.; Brendlé, M. Influence of Environment on the Size of the Elemental Wear Debris of Graphite. In *Boundary and Mixed Lubrication—Science and Applications, Proceedings ofthe 28th Leeds-Lyon Symposium on Tribology*; Dowson, D., Priest, M., Dalmaz, G., Lubrecht, A. A., Eds.; Elsevier, 2002; Vol. *40*, pp 295−304.
(10) Stempflé, P.; von Stebut, J. Nano-Mechanical Behaviour of the 3rd Body Generated in Dry Friction—Feedback Effect of the 3rd Body and Influence of the Surrounding Environment on the Tribology of Graphite. *Wear* **2006**, *260*, 601−614.
(11) Cabrera-Sanfelix, P.; Darling, G. R. Dissociative Adsorption of Water at Vacancy Defects in Graphite. *J. Phys. Chem. C* **2007**, *111*, 18258−18263.
(12) Jafary-Zadeh, M.; Reddy, C. D.; Zhang, Y.-W. Effect of Rotational Degrees of Freedom on Molecular Mobility. *J. Phys. Chem. C* **2013**, *117*, 6800−6806.
(13) Fouquet, P.; Johnson, M. R.; Hedgeland, H.; Jardine, A. P.; Ellis, J.; Allison, W. Molecular Dynamics Simulations of the Diffusion

DOI: 10.1021/acsami.9b13261
ACS Appl. Mater. Interfaces XXXX, XXX, XXX−XXX

of Benzene Sub-Monolayer Films on Graphite Basal Plane Surfaces. *Carbon* **2009**, *47*, 2627−2639.
(14) Allouche, A.; Ferro, Y. Dissociative Adsorption of Small Molecules at Vacancies on the Graphite (0001) Surface. *Carbon* **2006**, *44*, 3320−3327.
(15) Nevshupa, R. A.; Scherge, M.; Ahmed, S. I. U. Transitional Microfriction Behavior of Silicon Induced by Spontaneous Water Adsorption. *Surf. Sci.* **2002**, *517*, 17−28.
(16) Chen, L.; Chen, Z.; Tang, X.; Yan, W.; Zhou, Z.; Qian, L.; Kim, S. H. Friction at Single-Layer Graphene Step Edges Due to Chemical and Topographic Interactions. *Carbon* **2019**, *154*, 67−73.
(17) Vengudusamy, B.; Mufti, R. A.; Lamb, G. D.; Green, J. H.; Spikes, H. A. Friction Properties of DLC/DLC Contacts in Base Oil. *Tribol. Int.* **2011**, *44*, 922−932.
(18) Kirkhorn, L.; Gutnichenko, O.; Bihagen, S.; Ståhl, J.-E. Minimum Quantity Lubrication (MQL) with Carbon Nanostructured Additives in Sheet Metal Forming. *Procedia Manuf.* **2018**, *25*, 375−381.
(19) Huang, H. D.; Tu, J. P.; Gan, L. P.; Li, C. Z. An Investigation on Tribological Properties of Graphite Nanosheets as Oil Additive. *Wear* **2006**, *261*, 140−144.
(20) Zhang, Z.-c.; Cai, Z.-b.; Peng, J.-f.; Zhu, M.-h. Comparison of the Tribology Performance ofNano-Diesel Soot and Graphite Particles as Lubricant Additives. *J. Phys. D: Appl. Phys.* **2015**, *49*, No. 045304.
(21) Lancaster, J. K.; Pritchard, J. R. The Influence of Environment and Pressure on the Transition to Dusting Wear of Graphite. *J. Phys. D: Appl. Phys.* **1981**, *14*, 747−762.
(22) Buldum, A.; Lu, J. P. Atomic Scale Sliding and Rolling of Carbon Nanotubes. *Phys. Rev. Lett.* **1999**, *83*, 5050−5053.
(23) Calvo-Almazán, I.; Bahn, E.; Koza, M. M.; Zbiri, M.; Maccarini, M.; Telling, M. T. F.; Miret-Artés, S.; Fouquet, P. Benzene Diffusion on Graphite Described by a Rough Hard Disk Model. *Carbon* **2014**, *79*, 183−191.
(24) Calvo-Almazán, I.; Sacchi, M.; Tamtögl, A.; Bahn, E.; Koza, M. M.; Miret-Artés, S.; Fouquet, P. Ballistic Diffusion in Polyaromatic Hydrocarbons on Graphite. *J. Phys. Chem. Lett.* **2016**, *7*, 5285−5290.
(25) Kong, X.; Thomson, E. S.; Marković, N.; Pettersson, J. B. C. Dynamics and Kinetics of Methanol-Graphite Interactions at Low Surface Coverage. *ChemPhysChem* **2019**, *20*, 2171−2178.
(26) de Wijn, A. S. Internal Degrees of Freedom and Transport of Benzene on Graphite. *Phys. Rev. E* **2011**, *84*, No. 011610.
(27) Sader, J. E.; Larson, I.; Mulvaney, P.; White, L. R. Method for the Calibration of Atomic Force Microscope Cantilevers. *Rev. Sci. Instrum.* **1995**, *66*, 3789−3798.
(28) Barnette, A. L.; Asay, D. B.; Janik, M. J.; Kim, S. H. Adsorption Isotherm and Orientation of Alcohols on Hydrophilic SiO_2 under Ambient Conditions. *J. Phys. Chem. C* **2009**, *113*, 10632−10641.
(29) Barthel, A. J.; Luo, J.; Hwang, K. S.; Lee, J.-Y.; Kim, S. H. Boundary Lubrication Effect of Organic Residue Left on Surface After Evaporation of Organic Cleaning Solvent. *Wear* **2016**, *350*−*351*, 21−26.
(30) Senftle, T. P.; Hong, S.; Islam, M. M.; Kylasa, S. B.; Zheng, Y. X.; Shin, Y. K.; Junkermeier, C.; Engel-Herbert, R.; Janik, M. J.; Aktulga, H. M.; Verstraelen, T.; Grama, A.; van Duin, A. C. T. The ReaxFF Reactive Force-Field: Development, Applications and Future Directions. *npj Comput. Mater.* **2016**, *2*, No. 15011.
(31) Chipara, A. C.; Tsafack, T.; Owuor, P. S.; Yeon, J.; Junkermeier, C. E.; van Duin, A. C. T.; Bhowmick, S.; Asif, S. A. S.; Radhakrishnan, S.; Park, J. H.; Brunetto, G.; Kaipparettu, B. A.; Galvão, D. S.; Chipara, M.; Lou, J.; Tsang, H. H.; Dubey, M.; Vajtai, R.; Tiwary, C. S.; Ajayan, P. M. Underwater Adhesive Using Solid−Liquid Polymer Mixes. *Mater. Today Chem.* **2018**, *9*, 149−157.
(32) Goverapet Srinivasan, S.; van Duin, A. C. T. Molecular-Dynamics-Based Study of the Collisions of Hyperthermal Atomic Oxygen with Graphene Using the ReaxFF Reactive Force Field. *J. Phys. Chem. A* **2011**, *115*, 13269−13280.
(33) Chenoweth, K.; van Duin, A. C. T.; Goddard, W. A. ReaxFF Reactive Force Field for Molecular Dynamics Simulations of Hydrocarbon Oxidation. *J. Phys. Chem. A* **2008**, *112*, 1040−1053.
(34) Chenoweth, K.; Cheung, S.; van Duin, A. C. T.; Goddard, W. A.; Kober, E. M. Simulations on the Thermal Decomposition of a Poly(dimethylsiloxane) Polymer Using the ReaxFF Reactive Force Field. *J. Am. Chem. Soc.* **2005**, *127*, 7192−7202.
(35) Bauschlicher, C. W.; Qi, T.; Reed, E. J.; Lenfant, A.; Lawson, J. W.; Desai, T. G. Comparison of ReaxFF, DFTB, and DFT for Phenolic Pyrolysis. 2. Elementary Reaction Paths. *J. Phys. Chem. A* **2013**, *117*, 11126−11135.
(36) Qi, T.; Bauschlicher, C. W.; Lawson, J. W.; Desai, T. G.; Reed, E. J. Comparison of ReaxFF, DFTB, and DFT for Phenolic Pyrolysis. 1. Molecular Dynamics Simulations. *J. Phys. Chem. A* **2013**, *117*, 11115−11125.
(37) Qi, T.; Bauschlicher, C. W.; Lawson, J. W.; Desai, T. G.; Reed, E. J.; Lenfant, A. Addendum to "Comparison of ReaxFF, DFTB, and DFT for Phenolic Pyrolysis. 1. Molecular Dynamics Simulations" and "Comparison of ReaxFF, DFTB, and DFT for Phenolic Pyrolysis. 2. Elementary Reaction Paths". *J. Phys. Chem. A* **2014**, *118*, 5355−5357.
(38) Abadee, Z. G. N.; Hekmati, M.; Ganji, M. D. Removing Phenol Contaminants from Wastewater Using Graphene Nanobuds: DFT and Reactive MD Simulation Investigations. *J. Mol. Liq.* **2019**, *286*, No. 110872.
(39) Moradi, F.; Ganji, M. D.; Sarrafi, Y. Tunable Phenol Remediation from Wastewater Using SWCNT-Based, Sub-Nanometer Porous Membranes: Reactive Molecular Dynamics Simulations and DFT Calculations. *Phys. Chem. Chem. Phys.* **2017**, *19*, 8388−8399.
(40) O'Connor, T. C.; Andzelm, J.; Robbins, M. O. AIREBO-M: A Reactive Model for Hydrocarbons at Extreme Pressures. *J. Chem. Phys.* **2015**, *142*, No. 024903.
(41) Chen, Z.; Khajeh, A.; Martini, A.; Kim, S. H. Chemical and Physical Origins of Friction on Surfaces with Atomic Steps. *Sci. Adv.* **2019**, *5*, No. eaaw0513.
(42) Khajeh, A.; He, X.; Yeon, J.; Kim, S. H.; Martini, A. Mechanochemical Association Reaction of Interfacial Molecules Driven by Shear. *Langmuir* **2018**, *34*, 5971−5977.
(43) Barnette, A. L.; Asay, D. B.; Kim, D.; Guyer, B. D.; Lim, H.; Janik, M. J.; Kim, S. H. Experimental and Density Functional Theory Study of the Tribochemical Wear Behavior of SiO_2 in Humid and Alcohol Vapor Environments. *Langmuir* **2009**, *25*, 13052−13061.
(44) Plimpton, S. Fast Parallel Algorithms for Short-Range Molecular Dynamics. *J. Comput. Phys.* **1995**, *117*, 1−19.
(45) Stukowski, A. Visualization and Analysis of Atomistic Simulation Data with OVITO−the Open Visualization Tool. *Modell. Simul. Mater. Sci. Eng.* **2009**, *18*, No. 015012.
(46) Yaniv, R.; Koren, E. Robust Superlubricity of Gold−Graphite Heterointerfaces. *Adv. Funct. Mater.* **2019**, No. 1901138.
(47) Li, Q.; Dong, Y.; Perez, D.; Martini, A.; Carpick, R. W. Speed Dependence of Atomic Stick-Slip Friction in Optimally Matched Experiments and Molecular Dynamics Simulations. *Phys. Rev. Lett.* **2011**, *106*, No. 126101.
(48) Liu, X.-Z.; Ye, Z.; Dong, Y.; Egberts, P.; Carpick, R. W.; Martini, A. Dynamics of Atomic Stick-Slip Friction Examined with Atomic Force Microscopy and Atomistic Simulations at Overlapping Speeds. *Phys. Rev. Lett.* **2015**, *114*, No. 146102.
(49) Zaïdi, H.; Paulmier, D.; Lepage, J. The Influence of the Environment on the Friction and Wear of Graphitic Carbons: II. Gas Coverage of Wear Debris. *Appl. Surf. Sci.* **1990**, *44*, 221−233.
(50) Zaidi, H.; Robert, F.; Paulmier, D. Influence of Adsorbed Gases on the Surface Energy of Graphite: Consequences on the Friction Behaviour. *Thin Solid Films* **1995**, *264*, 46−51.
(51) Gao, G.; Mikulski, P. T.; Harrison, J. A. Molecular-Scale Tribology of Amorphous Carbon Coatings: Effects of Film Thickness, Adhesion, and Long-Range Interactions. *J. Am. Chem. Soc.* **2002**, *124*, 7202−7209.
(52) Marom, N.; Bernstein, J.; Garel, J.; Tkatchenko, A.; Joselevich, E.; Kronik, L.; Hod, O. Stacking and Registry Effects in Layered

DOI: 10.1021/acsami.9b13261
ACS Appl. Mater. Interfaces XXXX, XXX, XXX−XXX

Materials: the Case of Hexagonal Boron Nitride. *Phys. Rev. Lett.* **2010**, *105*, No. 046801.
(53) Hod, O. The Registry Index: a Quantitative Measure of Materials' Interfacial Commensurability. *ChemPhysChem* **2013**, *14*, 2376−91.
(54) Muraki, M. Molecular Structure of Synthetic Hydrocarbon Oils and Their Rheological Properties Governing Traction Characteristics. *Tribol. Int.* **1987**, *20*, 347−354.
(55) Toshiyuki, T.; Hitoshi, H. The Fundamental Molecular Structures of Synthetic Traction Fluids. *Tribol. Int.* **1994**, *27*, 183−187.
(56) Tsubouchi, T.; Hata, H. Study on the Fundamental Molecular Structures of Synthetic Traction Fluids: Part 2. *Tribol. Int.* **1995**, *28*, 335−340.
(57) Tamura, H.; Yoshida, M.; Kusakabe, K.; Chung; Miura, R.; Kubo, M.; Teraishi, K.; Chatterjee, A.; Miyamoto, A. Molecular Dynamics Simulation of Friction of Hydrocarbon Thin Films. *Langmuir* **1999**, *15*, 7816−7821.
(58) Ewen, J. P.; Gattinoni, C.; Zhang, J.; Heyes, D. M.; Spikes, H. A.; Dini, D. On the Effect of Confined Fluid Molecular Structure on Nonequilibrium Phase Behaviour and Friction. *Phys. Chem. Chem. Phy.* **2017**, *19*, 17883−17894.
(59) Molinari, R.; Poerio, T.; Argurio, P. One-Step Production of Phenol by Selective Oxidation of Benzene in a Biphasic System. *Catal. Today* **2006**, *118*, 52−56.
(60) Tomás-Pejó, E.; Alvira, P.; Ballesteros, M.; Negro, M. J. Pretreatment Technologies for Lignocellulose-to-Bioethanol Conversion. In *Biofuels*; Pandey, A., Larroche, C., Ricke, S. C., Dussap, C.-G., Gnansounou, E., Eds.; Academic Press: Amsterdam, 2011; Chapter 7, pp 149−176.
(61) Levitas, V. I.; Nesterenko, V. F.; Meyers, M. A. Strain-Induced Structural Changes and Chemical Reactions—I. Thermomechanical and Kinetic Models. *Acta Mater.* **1998**, *46*, 5929−5945.
(62) Koyama, M.; Hayakawa, J.; Onodera, T.; Ito, K.; Tsuboi, H.; Endou, A.; Kubo, M.; Del Carpio, C. A.; Miyamoto, A. Tribochemical Reaction Dynamics of Phosphoric Ester Lubricant Additive by Using a Hybrid Tight-Binding Quantum Chemical Molecular Dynamics Method. *J. Phys. Chem. B* **2006**, *110*, 17507−17511.
(63) Falk, M. L.; Langer, J. S. Dynamics of Viscoplastic Deformation in Amorphous Solids. *Phys. Rev. E* **1998**, *57*, 7192−7205.
(64) Shimizu, F.; Ogata, S.; Li, J. Theory of Shear Banding in Metallic Glasses and Molecular Dynamics Calculations. *Mater. Trans.* **2007**, *48*, 2923−2927.
(65) Yeon, J.; He, X.; Martini, A.; Kim, S. H. Mechanochemistry at Solid Surfaces: Polymerization of Adsorbed Molecules by Mechanical Shear at Tribological Interfaces. *ACS Appl. Mater. Interfaces* **2017**, *9*, 3142−3148.
(66) He, X.; Kim, S. H. Mechanochemistry of Physisorbed Molecules at Tribological Interfaces: Molecular Structure Dependence of Tribochemical Polymerization. *Langmuir* **2017**, *33*, 2717−2724.
(67) Barthel, A. J.; Combs, D. R.; Kim, S. H. Synthesis of Polymeric Lubricating Films Directly at the Sliding Interface via Mechanochemical Reactions of Allyl Alcohols Adsorbed from the Vapor Phase. *RSC Adv.* **2014**, *4*, 26081−26086.

DOI: 10.1021/acsami.9b13261
ACS Appl. Mater. Interfaces XXXX, XXX, XXX−XXX